Inorganic Chemistry

Article

pubs.acs.org/IC

How Can Multielectron Transfer Be Realized? A Case Study with Keggin-Type Polyoxometalates in Acetonitrile

Kazuo Eda* and Toshiyuki Osakai

Department of Chemistry, Graduate School of Science, Kobe University, Kobe 657-8501, Japan

Supporting Information

ABSTRACT: Theoretical consideration and computational simulation have been performed on the voltammetric properties of Keggin polyoxometalates (POMs), and the conversion from successive one-electron transfer in unacidified media to four-electron transfer (through two-electron transfer) in acidified media has been discussed. Perfect simulation of the cyclic voltammograms of POMs could be achieved using the standard formal potentials and the protonation constants, systematically evaluated by the equations, in which "simple (intrinsic)" and "synergistic (extrinsic)" electron-withdrawing effects of the μ_4-oxygen were taken into consideration. In the proposed model, the formal potential of the one-electron redox waves for the ith reduction step is presented by $E_i^\circ(z_0, s) = E_i^{**} + 0.51(z_0 - i + 1) + 1.067s$ (i = 1, 2, 3, 4; $E_1^{**} = E_2^{**} = 0.577$ V; $E_3^{**} = E_4^{**} = 0.377$ V), where z_0 is the initial ionic charge of a Keggin POM and s is the mean bond valence of the μ_4-O−W bonds in the POM. The values of E_i^{**}s are related to the energy levels of the two lowest unoccupied molecular orbitals (LUMOs) of a hypothetical Keggin POM with null charge and null bond valence. Then it was revealed that the LUMOs have small on-site repulsion, which may be an important factor that makes multielectron transfer feasible. These findings would give a big clue in developing novel redox materials exhibiting multielectron transfers.

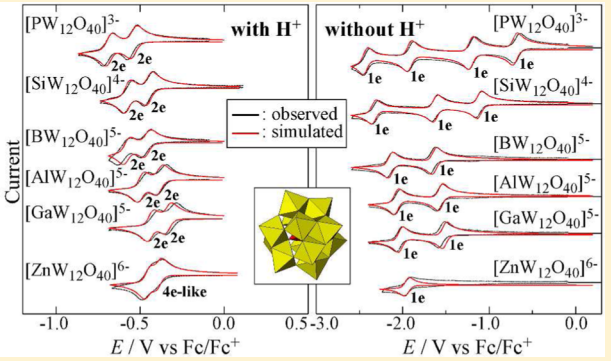

1. INTRODUCTION

Multielectron transfer is of major importance in a wide range of fields including renewable energy and biomimetic technologies.[1−3] Unlike one-electron transfer, multielectron transfer (especially more than two) is still a challenging subject. Keggin-type polyoxometalates (POMs) $[XM_{12}O_{40}]^z$ (M = Mo, W, V, Nb) possess a closed shell structure in the central cavity of which a variety of heteroatoms X having various formal charges (ranging from +6 to +2 for M = Mo, W) can be incorporated, as shown in Figure 1. Keggin POMs are stable in appropriate solvents and have ionic charge z widely ranging from −2 to −6 (for M = Mo, W). Therefore, they allow us to widely tune their physical properties (such as surface charge density and basicity) in terms of the heteroatom X, without changing their whole size and surface structure. Furthermore, Keggin POMs undergo multistep electron transfer without significantly deforming their shell framework and act as a reservoir of electrons. From these points of view, they are promising candidates for multielectron transfer materials and attract considerable interest in the areas of fundamental science and application technologies including catalysts, electron acceptors for photovoltaic devices, and antitumor or antiretroviral drugs.[4−7]

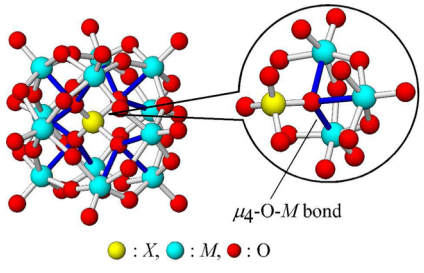

Figure 1. Structure of Keggin POM $[XM_{12}O_{40}]^{z_0}$.

Thus far the voltammetric properties of Keggin POMs have been extensively investigated.[5,8−11] It is known that they exhibit successive one-electron redox waves in unacidified aprotic solvents and that their first redox potentials depend linearly on their ionic charge. In acidified solvents the POMs undergo two-electron reductions, owing to the protonation of the reduced form at the electrode surface.[12−15] Moreover, Gao et al. reported that $[XMo_{12}O_{40}]^{6-}$ (X = Co^{II}, Ni^{II}) underwent four-electron transfers in acidified aqueous media.[16] Fundamental understanding of such multielectron processes is important to get a clue for developing novel potential materials exhibiting multielectron transfers.

In a preceding voltammetric and structural study on various tungsten Keggin-type POMs[17] it was found that their redox properties were governed not only by the ionic charge but also by the bond valence s of the μ_4-O−W bond (Figure 1). It was then revealed that $[ZnW_{12}O_{40}]^{6-}$ having a large bond valence s

Received: December 11, 2014
Published: March 5, 2015

DOI: 10.1021/ic502970q
Inorg. Chem. 2015, 54, 2793−2801

exhibited four-electron-like redox behavior in acidified media. To understand more about the relation between the bond valence s and the multielectron transfer, we herein performed theoretical consideration and computational simulation on their voltammetric properties and discussed the principles of the multistep one-electron reduction processes (up to four electron addition) and conversion from the successive one-electron reduction to two-electron or four-electron ones. Then perfect simulation of their cyclic voltammograms (CVs) was achieved by using a model involving a "synergistic" electron-withdrawing effect of the μ_4-oxygen and the attached protons, which would give a clue in developing redox materials exhibiting multielectron transfers.

2. EXPERIMENTAL SECTION

The experimental CVs of various Keggin tungstate anions were obtained in the previous study.[17] The measurements were carried out by using a conventional three-electrode system in which a glassy carbon disk electrode (area, 0.20 cm^2) was used as the working electrode. The test solution contained 0.50 mM Keggin anion in dry acetonitrile (water content < 50 ppm). The supporting electrolyte was $NaClO_4$ (0.10 M) for $[SW_{12}O_{40}]^{2-}$ and Bu_4NClO_4 (0.10 M) for the other Keggin POMs. For the acidification of solutions, CF_3SO_3H was added, so that the concentration became 10 mM. The voltage scan rate was usually 0.1 V/s^{-1}. The temperature of the test solution was kept at 25.0 °C ± 0.1 °C. In this paper all electrode potentials are reported with reference to the ferrocene/ferrocenium (Fc/Fc^+) couple.

The CVs were simulated using a simple explicit finite difference method.[18,19] In this simulation the redox processes considered were assumed to be reversible for simplicity. Calculation programs were originally written in Microsoft Visual Basic 6.0. Using the program, manual curve fitting of the experimental CVs with the simulated curves was performed to estimate a set of parameters, which include coefficients C_p^p and C_p^s for the z- and s-independent part and for the s-dependent part of the protonation energy of a Keggin POM, respectively, the diffusion coefficients of Keggin POMs and proton in the test solution, and the first protonation constant $K_{0,1}(z_0, s)$ of the oxidized form of the Keggin POM, which was used as a reference point for a systematic evaluation of the other protonation constants.

The bond valence s of the μ_4-O–W bond was calculated using the relationship $s = \exp[(d_0 - d)/B]$, where $d_0 = 1.917$, d = the μ_4-O–W bond length, and $B = 0.37$.[20] The bond lengths were determined from the crystallographic data of the corresponding crystals (see Table S1, Supporting Information).

3. RESULTS AND DISCUSSION

3.1. One-Electron Redox Behavior in Neutral Media.

3.1.1. Experimental Considerations of Simple Electron Transfer. In previous work it was found that the midpoint (formal) potential E_1 of the first redox wave of Keggin POMs depends on the (mean) bond valence s of the μ_4-O–W bonds as well as the ionic charge.[17] Since the electronegativity of oxygen (3.44) is greater than that of W (2.36), electrons may be drawn from the W atoms by the μ_4-oxygens, resulting in the depopulation of electrons on the W atoms and being used as bonding electrons of the μ_4-O–W bonds. This depopulation was also referred to by Mbomekallé et al., who studied the influence of the heteroatomic size on the redox potentials of Keggin anions.[21,22] The electron depopulation on the W atoms affects the redox potential E_1 due to the Coulomb repulsion between the electrons added and those originally populated on the W atom; thus, E_1 depends on s.[23] (For distinguishing from an additional, extrinsic electron-withdrawing effect mentioned below, we call this s-dependent effect the "simple (intrinsic)" electron-withdrawing effect of the μ_4-oxygen.) The plots of the E_1 values against the s value gave parallel straight lines, depending on the ionic charge of the POM, and the separation between the lines was 0.51 V per unit ionic charge (Figure S1, Supporting Information). This means that the E_1 value shifts to the negative potential side by 0.51 V per unit charge as the ionic charge z is negatively increased. In order to discuss the intrinsic effect of s on E_1 without the effect of ionic charge, we estimated the potentials E_1*s for a hypothetical Keggin POM with null charge and the valence s as $E_1^* = E_1 - 0.51z$, where E_1 is the potential for the Keggin POMs with charge z and the valence s. The plot of E_1* on s was linear, as reported previously (Figure 2).[17] The slope and intercept were 1.067 V per unit

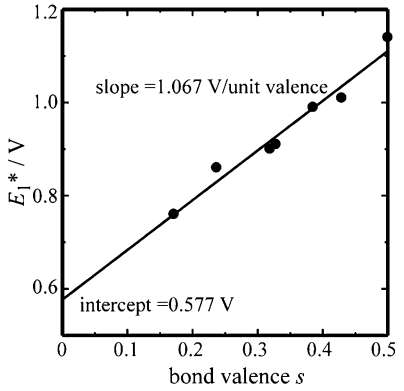

Figure 2. Plot of E_1* vs the bond valence s for $[XW_{12}O_{40}]^{z_0}$ ($z_0 = -2$ to -6). $E_1^* = E_1 - 0.51z_0$.

valence and 0.577 V, respectively, indicating that the first one-electron redox potential of the hypothetical Keggin POM with null charge and $s = 0$ is 0.577 V, and the formal potential shifts to positive potentials by 1.067 V per unit valence with increasing s.

In order to investigate if the other (i.e., the second to the fourth) redox waves also show the same dependence on the bond valence s, we compared the CVs recorded for different Keggin POMs, which were shown by using the electrode potential corrected for the bond-valence effect (i.e., $E_{corr} = E - 1.067s$) as in Figure 3 (original curves are shown in Figure 4). The first and second one-electron redox waves are correctly

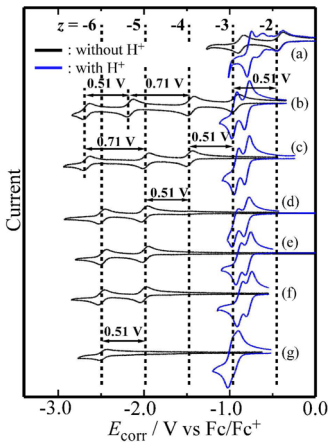

Figure 3. Cyclic voltammograms (black line, in neutral acetonitrile; blue line, in acidified acetonitrile) drawn vs E_{corr}: (a) $[SW_{12}O_{40}]^{2-}$, (b) $[PW_{12}O_{40}]^{3-}$, (c) $[SiW_{12}O_{40}]^{4-}$, (d) $[BW_{12}O_{40}]^{5-}$, (e) $[AlW_{12}O_{40}]^{5-}$, (f) $[GaW_{12}O_{40}]^{5-}$, and (g) $[ZnW_{12}O_{40}]^{6-}$. $E_{corr} = E - 1.067s$.

DOI: 10.1021/ic502970q
Inorg. Chem. 2015, 54, 2793–2801

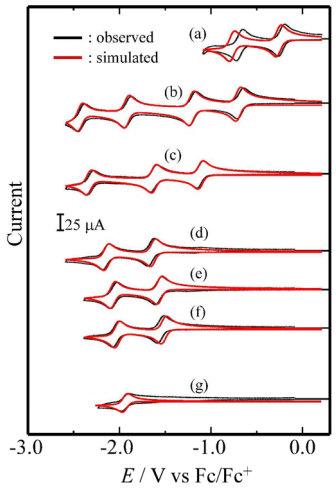

Figure 4. Cyclic voltammograms in neutral acetonitrile: observed (black line) and simulated (red line): (a) $[SW_{12}O_{40}]^{2-}$, (b) $[PW_{12}O_{40}]^{3-}$, (c) $[SiW_{12}O_{40}]^{4-}$, (d) $[BW_{12}O_{40}]^{5-}$, (e) $[AlW_{12}O_{40}]^{5-}$, (f) $[GaW_{12}O_{40}]^{5-}$, and (g) $[ZnW_{12}O_{40}]^{6-}$.

positioned on the corrected potential axis at an interval of 0.51 V depending on the ionic charge (of the prereduction form for the cathodic process or of the postoxidation form for the anodic process). However, the positions of the third and fourth waves are shifted from the expected positions by 0.2 V to negative potentials; this may be related to the energy difference between the first and the second lowest unoccupied molecular orbitals (LUMOs) or to their on-site repulsion, as mentioned below. Nevertheless, these results mean that the potentials of the second to fourth redox waves exhibit quite a similar dependence on the bond valence s as the first one does and further that the bond valence s remains unchanged even when at least four electrons are added to the POM. Thus, the formal potentials of the first four redox waves of the Keggin tungstate POMs are simply given by the following formula as a function of its initial ionic charge z_0 (i.e., the ionic charge that the oxidized form has), the bond valence s, and the ordinal number of redox reaction i, i.e.,

$$E_i^{\circ}(z_0, s) = E_i^{**} + 0.51(z_0 - i + 1) + 1.067s,\ i = 1, 2, 3, 4 \qquad (1)$$

where E_i^{**} is the formal potential of the ith redox wave of the hypothetical Keggin tungstate anion having null charge and null bond valence in the state preceding the corresponding redox reaction: E_1^{**} = 0.577 V, E_2^{**} = 0.577 V, E_3^{**} = 0.377 V, and E_4^{**} = 0.377 V. To verify eq 1, we simulated the CVs of various Keggin tungstate anions using the equation (Figure 4). The simulated CVs coincided well with the experimental ones except for the second wave of $[SW_{12}O_{40}]^{2-}$. This exceptional disagreement may be due to the ion pairing of the two-electron reduced anion with the supporting electrolyte cation, Na^+ (note that $NaClO_4$ instead of n-Bu_4NClO_4 was used only for $[SW_{12}O_{40}]^{2-}$, owing to its low solubility in the presence of n-Bu_4N^+). Thus, the quite good reproduction of the CVs by simulation demonstrates the validity of eq 1 and proves that the bond valence does not change during the first to fourth redox processes and that the second to fourth redox waves exhibit the same dependence on the bond valence s as the first one does. These findings are rather surprising because the valence and thus the redox behavior are affected by electron additions for common redox species. Precise understanding of the factors that determine the bond valence is not easy, but according to the characteristics of the central ion X (Table 1) it may be expressed roughly that the valence become larger as the radius

Table 1. Characteristics of the Central Cation X and the Mean Bond Valence s

X	z_0	ionic radii (pm)[a]	electronegativity[b]	s
S	−2	29	2.58	0.172
P	−3	34	2.19	0.237
Si	−4	40	1.90	0.328
B	−5	25	2.04	0.319
Al	−5	53	1.61	0.385
Ga	−5	61	1.81	0.429
Zn	−6	74	1.65	0.505

[a]The values were taken from the literature.[24,25] [b]The values were taken from the literature.[26]

of the central ion increases (i.e., in the case where a central oxoanion XO_4 is cooped up in the inner space of the Keggin shell with a fixed volume, as the central ion X becomes larger, the μ_4-oxygens coordinating to X are pushed more strongly against the W atoms on the Keggin shell and withdraw more electrons from the W atoms because of the greater electronegativity of the oxygens; then this leads to a larger bond valence of the μ_4-O−W bond). Since the sizes of the Keggin shell and the central XO_4 are unchanged during electron addition, the valence and redox behavior may thus remain unchanged.

3.1.2. Theoretical Consideration of Simple Electron Transfer. To understand theoretically the meaning of the above experimental findings, we try to discuss them electrothermodynamically. Let us consider the following four-step one-electron redox processes for a Keggin anion having initially an ionic charge z_0 and a bond valence s. The symbol $\langle n \rangle$ with n = 0, 1, 2, 3, or 4 indicates zero- (oxidized), one-, two-, three-, or four-electron reduced anion, respectively, namely, n is the number of electrons added to the Keggin POM. According to the above findings, the bond valence s is treated as unchanged during the following redox processes (Scheme 1).

Using the Gibbs energies of hypothetical successive reaction processes (including desolvation, electron gaining in the standard gaseous state, and solvation), we can write the standard redox potentials E°'s for the respective redox steps as

$$E_1^{\circ}(z_0, s) = \frac{-1}{F}\{\Delta G_{eg}^{\circ}(\langle 0 \rangle_s^{z_0}) + \Delta G_{solv}^{\circ}(\langle 1 \rangle_s^{z_0-1}) - \Delta G_{solv}^{\circ}(\langle 0 \rangle_s^{z_0})\} - E_{ref} \qquad (2)$$

$$E_2^{\circ}(z_0, s) = \frac{-1}{F}\{\Delta G_{eg}^{\circ}(\langle 1 \rangle_s^{z_0-1}) + \Delta G_{solv}^{\circ}(\langle 2 \rangle_s^{z_0-2}) - \Delta G_{solv}^{\circ}(\langle 1 \rangle_s^{z_0-1})\} - E_{ref} \qquad (3)$$

$$E_3^{\circ}(z_0, s) = \frac{-1}{F}\{\Delta G_{eg}^{\circ}(\langle 2 \rangle_s^{z_0-2}) + \Delta G_{solv}^{\circ}(\langle 3 \rangle_s^{z_0-3}) - \Delta G_{solv}^{\circ}(\langle 2 \rangle_s^{z_0-2})\} - E_{ref} \qquad (4)$$

$$E_4^{\circ}(z_0, s) = \frac{-1}{F}\{\Delta G_{eg}^{\circ}(\langle 3 \rangle_s^{z_0-3}) + \Delta G_{solv}^{\circ}(\langle 4 \rangle_s^{z_0-4}) - \Delta G_{solv}^{\circ}(\langle 3 \rangle_s^{z_0-3})\} - E_{ref} \qquad (5)$$

where ΔG_{eg}° and ΔG_{solv}° are, respectively, the standard Gibbs energies of electron gaining and of solvation for the Keggin

DOI: 10.1021/ic502970q
Inorg. Chem. 2015, 54, 2793−2801

Scheme 1. Redox Processes in Unacidified Media

$$\langle 0\rangle_s^{z_0} \underset{-e}{\overset{+e}{\rightleftharpoons}} \langle 1\rangle_s^{z_0-1} \underset{-e}{\overset{+e}{\rightleftharpoons}} \langle 2\rangle_s^{z_0-2} \underset{-e}{\overset{+e}{\rightleftharpoons}} \langle 3\rangle_s^{z_0-3} \underset{-e}{\overset{+e}{\rightleftharpoons}} \langle 4\rangle_s^{z_0-4}$$
$$E_1 \qquad E_2 \qquad E_3 \qquad E_4$$

anion given in parentheses and E_{ref} is the reference-electrode potential employed. These equations can be written generally as follows

$$E_i^\circ(z_0, s) = \frac{-1}{F}\{\Delta G_{eg}^\circ(\langle i-1\rangle_s^{z_0-i+1}) + \Delta G_{solv}^\circ(\langle i\rangle_s^{z_0-i}) - \Delta G_{solv}^\circ(\langle i-1\rangle_s^{z_0-i+1})\} - E_{ref},\ i = 1, 2, 3, 4 \quad (6)$$

Because ΔG_{eg}° is concerned with the energy that can be extracted when an electron is added to a Keggin anion, the energies for the present four one-electron redox reactions depend on the energy levels of (at least two) LUMOs, which are related to the tungsten d orbitals as mentioned below. They are also concerned with the energy of the Coulomb interaction between the electron added and the ionic charge z. Moreover, as we suggested in section 3.1.1, the Coulomb interaction of the electron added is affected by partial depopulation of the electron on the W atoms, concerned with the bond valence s of the μ_4-O−W (the simple electron-withdrawing effect of the μ_4-oxygen). Thus, ΔG_{eg}° is described as

$$\Delta G_{eg}^\circ = \Delta G_{eg}^{\circ\,orb} + \Delta G_{eg}^{\circ z} + \Delta G_{eg}^{\circ s} \quad (7)$$

where $\Delta G_{eg}^{\circ\,orb}$ is the z- and s-independent term that is related to the energy states of the molecular orbitals of the Keggin POM (to be exact, those of the hypothetical POM with null charge and null bond valence) and $\Delta G_{eg}^{\circ z}$ and $\Delta G_{eg}^{\circ s}$ are, respectively, the z- and s-dependent terms, which are both concerned with the Coulomb interaction energy. The z-dependent term $\Delta G_{eg}^{\circ z}$ can be formulated as[27]

$$\Delta G_{eg}^{\circ z} \propto -N_A z e^2/4\pi\varepsilon_0 r \quad (8)$$

where N_A and ε_0 are Avogadro's number and the electric permittivity of a vacuum and r is the radius of the Keggin POM that is regarded as a constant independent of the kind of central heteroatom. In the present discussion, however, this term is simply formulated for a $\langle n\rangle^{z_0-n}$ anion as

$$\Delta G_{eg}^{\circ z}(\langle n\rangle^{z_0-n}) = -C_{eg}^z\cdot z = -C_{eg}^z\cdot(z_0 - n),\ n = 0, 1, 2, 3, 4 \quad (8')$$

where C_{eg}^z is a coefficient common to all Keggin tungstate anions, giving the change in the electron-gaining Gibbs energy per unit charge. Since $\Delta G_{eg}^{\circ s}$ is the s-dependent term and related to the Coulomb interaction energy similar to $\Delta G_{eg}^{\circ z}$ it is given as

$$\Delta G_{eg}^{\circ s}(\langle n\rangle_s) = -C_{eg}^s\cdot s \quad (9)$$

where C_{eg}^s is also a common coefficient that gives the change in the electron-gaining Gibbs energy per unit bond valence.

Since total ionic charge is independent of the bond valence s, ΔG_{solv}° is treated to be independent of s. Recently, we have shown that the hydration energy of a spherical ion scaled by the surface area can be well expressed by a quadratic equation of the surface field strength (E_{sf}) of the ion.[28] Extending this equation to the solvation energy of a Keggin POM in the nonaqueous solvent (i.e., acetonitrile), we herein assume that $\Delta G_{solv}^\circ(\langle n\rangle^{z_0-n})$ scaled by the surface area ($4\pi r^2$) is given by

$$\frac{\Delta G_{solv}^\circ(\langle n\rangle^{z_0-n})}{4\pi r^2} = -aE_{sf}^2 - bE_{sf} - c \quad (10)$$

where the coefficients, a, b, and c, include the parameters regarding the short-range ion−solvent interactions (e.g., the dipole moment and electron polarizability of the solvent molecule and the parameters concerned with the charge-transfer (CT) interaction, etc.).[28] It should be noted that eq 10 was successfully derived by neglecting the Born-type, long-range ion−solvent interaction,[29] since its contribution to the total solvation energy is very small compared with that of the short-range interaction. By here considering that E_{sf} for a spherical ion is given by $E_{sf} = ze/4\pi\varepsilon_0 r^2$, eq 10 is rewritten as

$$\Delta G_{solv}^\circ(\langle n\rangle^{z_0-n}) = \Delta G_{solv}^\circ(\langle n\rangle^z) = -a'z^2 - b'z - c' \quad (10')$$

The z-independent term $\Delta\bar{G}_{solv}^\circ(\langle n\rangle)$ ($= -c'$) is mainly concerned with the energy of the formation of a cavity in solvent. Since the POM size does not change, $\Delta\bar{G}_{solv}^\circ(\langle n\rangle)$ is regarded as a constant independent of n being expressed as

$$\Delta\bar{G}_{solv}^\circ(\langle n\rangle) = -C_{solv}^{cav} \quad (11)$$

On the other hand, the z-dependent term $\Delta\bar{G}_{solv}^{\circ z}(\langle n\rangle^{z_0-n})$ ($= -a'z^2 - b'z$) is rewritten by changing the coefficients a' and b' into C_{solv}^{z2} and C_{solv}^{z1}, respectively, as

$$\Delta G_{solv}^{\circ z}(\langle n^{z_0-n}\rangle) = -C_{solv}^{z2}\cdot z^2 - C_{solv}^{z1}\cdot z = -C_{solv}^{z2}\cdot(z_0 - n)^2 - C_{solv}^{z1}\cdot(z_0 - n) \quad (12)$$

Although we used this equation in the present work, it should be noted that similar conclusions shown below are obtainable even when using the Born-like free energy of solvation (with $C_{solv}^{z1} = 0$) instead of the above non-Bornian solvation energy $\Delta G_{solv}^{\circ z}$.

Introducing eqs 7, 8′, 9, 11, and 12 into eq 6 gives

$$E_i^\circ(z_0, s) = \frac{-1}{F}\{(\Delta G_{eg}^{\circ\,orb}(\langle i-1\rangle) - C_{solv}^{z2} + C_{solv}^{z1}) - (C_{eg}^z - 2C_{solv}^{z2})(z_0 - i + 1) - C_{eg}^s\cdot s\} - E_{ref},\ i = 1, 2, 3, 4 \quad (13)$$

Comparison of eq 13 with eq 1 shows

$$E_1^{**} = \frac{-1}{F}(\Delta G_{eg}^{\circ\,orb}(\langle 0\rangle) - C_{solv}^{z2} + C_{solv}^{z1}) - E_{ref} = 0.577\text{V} \quad (14)$$

$$E_2^{**} = \frac{-1}{F}(\Delta G_{eg}^{\circ\,orb}(\langle 1\rangle) - C_{solv}^{z2} + C_{solv}^{z1}) - E_{ref} = 0.577\text{V} \quad (15)$$

$$E_3^{**} = \frac{-1}{F}(\Delta G_{eg}^{\circ\,orb}(\langle 2\rangle) - C_{solv}^{z2} + C_{solv}^{z1}) - E_{ref} = 0.377\text{V} \quad (16)$$

$$E_4^{**} = \frac{-1}{F}(\Delta G_{eg}^{\circ\,orb}(\langle 3\rangle) - C_{solv}^{z2} + C_{solv}^{z1}) - E_{ref} = 0.377\text{V} \quad (17)$$

DOI: 10.1021/ic502970q
Inorg. Chem. 2015, 54, 2793−2801

$$C^{z}_{eg} - 2C^{z2}_{solv} = 0.51F \quad (18)$$

$$C^{s}_{eg} = 1.067F \quad (19)$$

Since the term $(-1/F)(-C^{z2}_{solv} + C^{z1}_{solv}) - E_{ref}$ is common, eqs 14−17 give relative relations among the $\Delta G^{oorb}_{eg}(\langle n \rangle)$'s that correspond to the four lowest energy states concerning the two LUMOs of the hypothetical Keggin POM with null charge and null bond valence. The relations $E_1^{**} = E_2^{**} = 0.577$ V and $E_3^{**} = E_4^{**} = 0.377$ V show that the first and second electrons occupy the orbitals lying at the same level, while the third and fourth electrons occupy the orbitals lying at a level higher by 0.2 eV than the levels of the first and second electrons. From the point symmetry (T_d) of the Keggin $W_{12}O_{36}$ shell where the bridging O−W bonds (along x or y axis) are longer than the terminal bonds, its LUMO consists of T_d symmetry-adapted combinations of the d_{xy}-like orbitals and is a doubly degenerate one of symmetry e.[30] Accordingly, it is suggested at first that the first and second electrons occupy the doubly degenerate orbitals adopting a high-spin configuration (with parallel spins according to Hund's first rule) and then the third and fourth electrons occupy the same orbitals with spins antiparallel to those of the first two electrons showing an energy difference of 0.2 eV due to the on-site repulsion,[31] as depicted in Figure 5a.

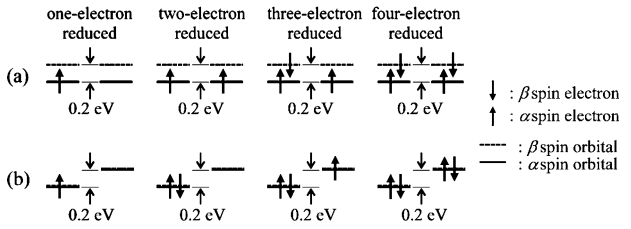

Figure 5. Electron configurations of one-, two-, three-, and four-electron reduced Keggin anions: (a) doubly degenerated LUMO model and (b) split LUMO model.

This suggestion, however, does not account for the known fact that the two-electron reduced Keggin POM exhibits diamagnetism (due to a low-spin configuration for the added two electrons).[32] Therefore, an alternative model has finally been suggested in which the doubly degenerate LUMO is further split into two different levels separated by 0.20 eV, owing to some reason such as symmetry breaking in a real anion, and the four added electrons occupy sequentially the two split levels from the bottom adopting a low-spin configuration (Figure 5b). In this case the on-site repulsion is not large and regarded equal to off-site repulsion.[31] Such small on-site repulsion may be due to the properties of the corresponding orbitals widely spread on 12 W atoms of the Keggin POM. Also, the close energy levels and the small on-site repulsion of LUMOs (or LUMO+1) of the Keggin POMs may be important factors that make four-electron transfer feasible.

3.2. Multielectron Redox Behavior in Acidified Media.

3.2.1. Experimental Considerations of Electron Transfer Accompanied by Protonation. It is known that $[XW_{12}O_{40}]^{z_0}$ (with z_0 ranging from −3 to −6) undergoes two-electron reduction accompanied by consumption of protons in acidified media (i.e., successive four elementary one-electron redox waves turn to two two-electron ones).[12−15,17] In our previous study no correlation of their formal potentials with ionic charge was observed in acidified media, unlike in unacidified media. However, when the CVs were drawn on the E_{corr} axis (corrected for the bond valence effect), all two-electron redox waves are positioned around the electrode potential where the first one-electron redox wave of the Keggin POM with an initial ionic charge of −3 appears (Figure 3). This probably means that in the acidified media the Keggin tungstate anions having ionic charges negatively larger than −3 exhibit protonation and their reduction is always accompanied by protonation, keeping their overall ionic charge constant at −3. It is thus suggested that the discorrelation of the formal potential with the ionic charge, being observed in acidified media, is due to the constant overall ionic charge, resulting from the protonation.

Furthermore, the first and second formal potentials, E_1^p and E_2^p, of the two two-electron waves involving protonation showed linear dependences on the s value.[17] However, the two-electron waves became closer as s became larger, and ultimately they were merged into a four-electron-like wave for $[XW_{12}O_{40}]^{6-}$ (X = Zn^{II}) with the biggest bond valence s (Table 2 and Figure 6). This means that the first and second

Table 2. Peak Separation between the Two Two-Electron Redox Waves

X	z_0	s	m_{2e}[a]	m_{4e}[b]	ΔE (V)[c]
S	−2	0.172	1	3	(two 1e + one 2e)[d]
P	−3	0.237	2	4	0.15
Si	−4	0.328	3	5	0.12
B	−5	0.319	4	6	0.12
Al	−5	0.385	4	6	0.11
Ga	−5	0.429	4	6	0.10
Zn	−6	0.505	5	7	(one 4e)[e]

[a]The number of attached protons, expected for a two-electron reduced POM. [b]The number of attached protons, expected for a four-electron reduced POM. These numbers were determined so as to keep the overall ionic charge constant at −3. [c]The peak separation between the two two-electron redox waves, obtained from the anodic peak potentials. [d]Two one-electron and one two-electron redox waves are observed. [e]One four-electron-like redox wave is observed.

two-electron waves depend with different degrees on the bond valence s in acidified media and that the number m of protons attached on the Keggin anion and/or the redox state of the

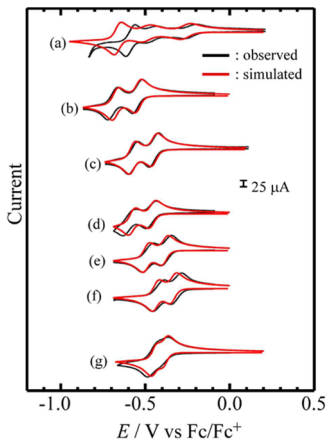

Figure 6. Cyclic voltammograms in acidified acetonitrile: observed (black line) and simulated (red line): (a) $[SW_{12}O_{40}]^{2-}$, (b) $[PW_{12}O_{40}]^{3-}$, (c) $[SiW_{12}O_{40}]^{4-}$, (d) $[BW_{12}O_{40}]^{5-}$, (e) $[AlW_{12}O_{40}]^{5-}$, (f) $[GaW_{12}O_{40}]^{5-}$, and (g) $[ZnW_{12}O_{40}]^{6-}$. The values of C^p_p and C^s_p used for these simulation are $0.015F$ and $0.007F$, respectively.

DOI: 10.1021/ic502970q
Inorg. Chem. 2015, 54, 2793−2801

Keggin POM (i.e., n, the number of electrons added to the Keggin anion) affect the potential shift due to the bond valence s (Table 2). Thus, it is of importance to investigate what the energy effect leading to this additional s dependence is and how it is described by s and n and/or m.

3.2.2. Theoretical Considerations of Electron Transfer Accompanied by Protonation. Since a formal potential E_i^{p} of a two-electron redox wave is determined by two successive "elementary" (one-electron) redox reactions that accompany protonation, the redox behavior in acidified media is discussed in terms of the redox potentials ${}^{\mathrm{e}}E_i^{\mathrm{p}}$'s of these elementary reactions. Thus, let us consider the following elementary (one-electron) redox and subsequent protonation steps, shown in Scheme 2.

Scheme 2. Redox Processes in Acidified Media

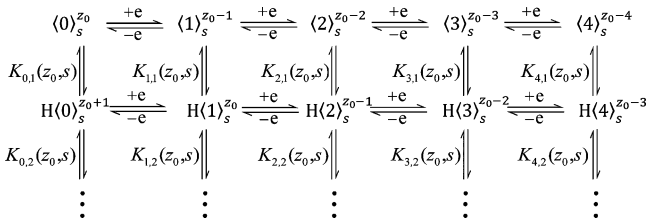

The protonation constants should be dependent on z_0 and s and denoted by $K_{n,m}(z_0, s)$ with n = 0, 1, 2, 3, 4 and m = 1, 2, 3,... In a reversible system, where all redox processes are fast, the electrode potential E is given by using the concentrations of all relevant redox species at the electrode surface as

$$E = {}^{\mathrm{e}}E_i^{\mathrm{p}\circ}(z_0, s) + \frac{RT}{F}\ln\frac{[\langle i-1\rangle_s^{z_0-i+1}] + [\mathrm{H}\langle i-1\rangle_s^{z_0-i+2}] + [\mathrm{H}_2\langle i-1\rangle_s^{z_0-i+3}]\ldots}{[\langle i\rangle_s^{z_0-i}] + [\mathrm{H}\langle i\rangle_s^{z_0-i+1}] + [\mathrm{H}_2\langle i\rangle_s^{z_0-i+2}] + \ldots} \quad (20)$$

where ${}^{\mathrm{e}}E_i^{\mathrm{p}\circ}(z_0, s)$ is the apparent standard formal potential, which is described in terms of the concentration of proton, protonation constants, and standard redox potentials of unprotonated species as

$${}^{\mathrm{e}}E_i^{\mathrm{p}\circ}(z_0, s) = E_i^{\circ}(z_0, s) + \frac{RT}{F}\ln\frac{1 + K_{i,1}(z_0, s)[\mathrm{H}^+] + K_{i,1}(z_0, s)[\mathrm{H}^+]^2 + \ldots}{1 + K_{i-1,1}(z_0, s)[\mathrm{H}^+] + K_{i-1,1}(z_0, s)[\mathrm{H}^+]^2 + \ldots} \quad (21)$$

Furthermore, the protonation constants are related to the Gibbs energy of protonation in the standard solution state, being given by using the Gibbs energy of protonation in the standard gaseous state $\Delta G_{\mathrm{p}}^{\circ}$ and solvation (and desolvation) Gibbs energies needed to convert the gaseous state to the solution state (and vice versa) as follows

$$-RT\ln K_{n,m}(z_0, s) = \Delta G_{\mathrm{p}}^{\circ}(\mathrm{H}_m\langle n\rangle_s^{z_0-n+m}) + \Delta G_{\mathrm{solv}}^{\circ}(\mathrm{H}_m\langle n\rangle_s^{z_0-n+m}) - \Delta G_{\mathrm{solv}}^{\circ}(\mathrm{H}_{m-1}\langle n\rangle_s^{z_0-n+m-1}) - \Delta G_{\mathrm{solv}}^{\circ}(\mathrm{H}^+) \quad (22)$$

Protonation can be regarded as a charged-particle-gaining process like the electron gaining of a POM anion. Therefore, the standard Gibbs energy of protonation $\Delta G_{\mathrm{p}}^{\circ}$ is here given in a similar manner as $\Delta G_{\mathrm{eg}}^{\circ}$ (eq 7) by a function of z and s

$$\Delta G_{\mathrm{p}}^{\circ} = \Delta\bar{G}_{\mathrm{p}}^{\circ} + \Delta G_{\mathrm{p}}^{\circ z} + \Delta G_{\mathrm{p}}^{\circ s} \quad (23)$$

where $\Delta\bar{G}_{\mathrm{p}}^{\circ}$ is a z- and s-independent part of the interaction between the attached proton and the Keggin anion and may depend on the chemical structure of the anion's surface (being affected by protons attached prior to the protonation step of interest). Thus, the $\Delta\bar{G}_{\mathrm{p}}^{\circ}$ for a protonated anion, $\mathrm{H}_m\langle n\rangle$, is given as

$$\Delta\bar{G}_{\mathrm{p}}^{\circ}(\mathrm{H}_m\langle n\rangle) = -\bar{C}_{\mathrm{p}}^{\mathrm{bs}} - C_{\mathrm{p}}^{\mathrm{p}}\cdot(m-1),\ m = 1, 2, 3, \ldots \quad (24)$$

where $\bar{C}_{\mathrm{p}}^{\mathrm{bs}}$ and $C_{\mathrm{p}}^{\mathrm{p}}$ are the coefficients that describe the contributions due to the bare surface of the Keggin anion and due to the protons attached on the surface, respectively. In eq 23, $\Delta G_{\mathrm{p}}^{\circ z}$ is a z-dependent term and formulated for a $\mathrm{H}_m\langle n\rangle^{z_0-n+m}$ anion as[33]

$$\Delta G_{\mathrm{p}}^{\circ z}(\mathrm{H}_m\langle n\rangle^{z_0-n+m}) = C_{\mathrm{p}}^{z}\cdot(z-1) = C_{\mathrm{p}}^{z}\cdot(z_0-n+m-1) \quad (25)$$

This equation describes a Coulomb interaction similar to that of electron gaining (eq 8′), which however has a plus sign because of the positive charge of the proton. Also, $\Delta G_{\mathrm{p}}^{\circ s}$ in eq 23 is a s-dependent term and should be concerned with the s dependence of the first and second two-electron redox waves (to be exact, the s dependence of the first to fourth elementary redox waves, accompanied by protonation processes). Thus, this term is a function of m and/or n as well as s, because the degree of the s dependence seems to vary with m and/or n, as mentioned in section 3.2.1. If the s dependence is simply owing to the Coulomb interaction between the proton attached and the effective positive charge on a W atom resulting from the electron depopulation,[34] which depends on s, $\Delta G_{\mathrm{p}}^{\circ s}$ should be positive to result in the suppression of electron transfer. However, the acceleration of electron transfer is needed for the occurrence of multielectron transfers observed (i.e., $\Delta G_{\mathrm{p}}^{\circ s}$ should be negative). Because protons attach to the surface oxygen atoms connected to W atoms,[35] they would affect the depopulation of electrons on the W atoms by the μ_4-oxygen. Then, as a possible factor for the acceleration of electron transfer, we propose a "synergistic" electron-withdrawing effect by the bond valence s (or the μ_4-oxygen) and the attached protons, that is, (1) the μ_4-oxygen and the attached protons synergistically withdraw electrons from the W atoms, yielding an additional effective positive charge on the W atoms, the magnitude of which may be described as proportional to a product of s and the number m of protons attached, and (2) the Coulomb interaction between the resulting effective positive charge and the n electrons added by reduction lowers the formation (or protonation) Gibbs energy of the $\mathrm{H}_m\langle n\rangle_s$ anion and thus results in the acceleration of protonation (consequently, the acceleration of electron transfer). Considering the effect, we tested various types of formulas expressing the dependence of $\Delta G_{\mathrm{p}}^{\circ s}(\mathrm{H}_m\langle n\rangle_s)$ on m, n, and s. Using the following formula, the best fit of CVs was obtained by digital simulation.

$$\Delta G_{\mathrm{p}}^{\circ s}(\mathrm{H}_m\langle n\rangle_s) = -C_{\mathrm{p}}^{s}\cdot m\cdot s\cdot n \quad (26)$$

Other types of formulas were also used, but less satisfactory simulation results were obtained as discussed below.

Furthermore, to minimize the number of fitting parameters for the simulation, we obtained an important relation between

DOI: 10.1021/ic502970q
Inorg. Chem. 2015, 54, 2793−2801

C_p^z and C_{eg}^z from the thermodynamic necessity that the overall Gibbs energy change is independent of the reaction routes (i.e., independent of whether electron gaining is prior or posterior to protonation). The necessity is expressed as

$$\Delta G_p^\circ(H_m\langle n\rangle_s^{z_0-n+m}) + \Delta G_{eg}^\circ(H_m\langle n\rangle_s^{z_0-n+m}) = \Delta G_{eg}^\circ(H_{m-1}\langle n\rangle_s^{z_0-n+m-1}) + \Delta G_p^\circ(H_m\langle n+1\rangle_s^{z_0-n+m-1});\ n = 0, 1, 2, 3;\ m = 1, 2, \ldots \quad (27)$$

Introducing eqs 7, 8′, 9, 11, 12, 18, and 23−26 into eq 27, we obtain

$$\Delta G_{eg}^{\circ orb}(H_m\langle n\rangle) - \Delta G_{eg}^{\circ orb}(H_{m-1}\langle n\rangle) + \Delta G_{eg}^{os}(H_m\langle n\rangle_s) - \Delta G_{eg}^{os}(H_{m-1}\langle n\rangle_s) + C_p^s\cdot m\cdot s = C_{eg}^z - C_p^z \quad (27')$$

Since this equation should be satisfied for every reaction step in Scheme 2, independent of the values of m, n, and s, we can assume that the left-hand side of eq 27′ is zero.

Consequently, eq 27′ simply turns to

$$C_p^z = C_{eg}^z \quad (27'')$$

This equation seems reasonable because a proton and an electron are both unit-charged particles and concern a charge-cancellation effect among the transferring or gained particles.

To evaluate all protonation constants systematically, we formulated the following terms involving protonation constants

$$(1)\ RT\ln\frac{K_{0,1}(z_0+1,s)}{K_{0,1}(z_0,s)},\ (2)\ RT\ln\frac{K_{n+1,m}(z_0,s)}{K_{n,m}(z_0,s)},\ \text{and}\ (3)\ RT\ln\frac{K_{n,m+1}(z_0,s)}{K_{n,m}(z_0,s)}$$

By using eq 22, these terms are given as follows

$$(1)\ RT\ln\frac{K_{0,1}(z_0+1,s)}{K_{0,1}(z_0,s)} = -\Delta G_p^\circ(H\langle 0\rangle_s^{z_0+1}) + \Delta G_p^\circ(H\langle 0\rangle_s^{z_0}) - \Delta G_{solv}^\circ(H\langle 0\rangle_s^{z_0+2}) + \Delta G_{solv}^\circ(H\langle 0\rangle_s^{z_0+1}) + \Delta G_{solv}^\circ(\langle 0\rangle_s^{z_0+1}) - \Delta G_{solv}^\circ(\langle 0\rangle_s^{z_0}) \quad (28)$$

Here, the ΔG_{solv}° terms are given by eq 11 and their z-independent term $\Delta\bar{G}_{solv}^\circ$ should be affected by the protonation of the POM anion and has thus been assumed to depend on the number m of the protons attached on the anionic surface, i.e.,

$$\Delta\bar{G}_{solv}^\circ(H_m\langle n\rangle) = -C_{solv}^{cav} - C_{solv}^p\cdot m \quad (11')$$

By introducing eqs 11′, 18, 23−26, and 27″ into eq 28, we finally obtain

$$RT\ln\frac{K_{0,1}(z_0+1,s)}{K_{0,1}(z_0,s)} = C_p^z\cdot 1 - 2C_{sol}^{z2}\cdot I^2 = C_{eg}^z - 2C_{sol}^{z2} = 0.51F \quad (28')$$

$$(2)\ RT\ln\frac{K_{n+1,m}(z_0,s)}{K_{n,m}(z_0,s)} = -\Delta G_p^\circ(H_m\langle n+1\rangle_s^{z_0-n+m-2}) + \Delta G_p^\circ(H_m\langle n\rangle_s^{z_0-n+m-1}) - \Delta G_{solv}^\circ(H_m\langle n+1\rangle_s^{z_0-n+m-1}) + \Delta G_{solv}^\circ(H_m\langle n\rangle_s^{z_0-n+m}) + \Delta G_{solv}^\circ(H_{m-1}\langle n+1\rangle_s^{z_0-n+m-2}) - \Delta G_{solv}^\circ(H_{m-1}\langle n\rangle_s^{z_0-n+m-1}) \quad (29)$$

By introducing eqs 11′, 18, 23−26, and 27″ into eq 29, we obtain

$$RT\ln\frac{K_{n+1,m}(z_0,s)}{K_{n,m}(z_0,s)} = C_p^z\cdot 1 - 2C_{sol}^{z2}\cdot I^2 - C_p^s\cdot m\cdot s\cdot 1 = 0.51F + C_p^s\cdot m\cdot s \quad (29')$$

$$(3)\ RT\ln\frac{K_{l,m+1}(z_0,s)}{K_{n,m}(z_0,s)} = -\Delta G_p^\circ(H_{m+1}\langle n\rangle_s^{z_0-n+m}) + \Delta G_p^\circ(H_m\langle n\rangle_s^{z_0-n+m-1}) - \Delta G_{solv}^\circ(H_{m+1}\langle n\rangle_s^{z_0-n+m+1}) + \Delta G_{solv}^\circ(H_m\langle n\rangle_s^{z_0-n+m}) + \Delta G_{solv}^\circ(H_m\langle n\rangle_s^{z_0-n+m}) - \Delta G_{solv}^\circ(H_{m-1}\langle n\rangle_s^{z_0-n+m-1}) \quad (30)$$

Introducing eqs 11′, 18, 23−26, and 27″ into eq 30 shows

$$RT\ln\frac{K_{n,m+1}(z_0,s)}{K_{n,m}(z_0,s)} = C_p^p\cdot 1 + C_p^s\cdot 1\cdot s\cdot n - C_p^z\cdot 1 + 2C_{sol}^{z2}\cdot I^2 = C_p^p + C_p^s\cdot s\cdot n - 0.51F \quad (30')$$

On the basis of eqs 20 and 21, we digitally simulated the CVs observed for the Keggin anions in acidified acetonitrile. The protonation constants calculated systematically by the above generalized relations (eqs 28′, 29′, and 30′) and the standard redox potentials given by eq 1 were used in the simulation. At first, to fit the CVs observed, only three values of $K_{0,1}(-4, s)$, C_p^p, C_p^s were adjusted as fitting parameters common to all Keggin tungsten POMs studied.[36] Use of proper values for C_p^p and C_p^s gave good reproduction of the redox behaviors (i.e., the shape of the CVs) of the Keggin tungstate POMs where the two two-electron waves come close and merge into a four-electron-like wave as the bond valence s becomes larger. Reproduction of peak positions in the CVs, however, was not fully achieved. Displacement between the observed and the calculated peak positions became larger as the value of z_0 is apart more from −4. For full reproduction, some modifications of $K_{0,1}(z_0, s)$'s from the values calculated with eq 28′ were needed. According to eq 26, $\Delta G_p^{os}(H_m\langle n\rangle_s) = 0$ when $n = 0$ (i.e., $K_{0,1}(z_0, s)$ should be regarded as a function only of z_0, differing from the other $K_{n,m}(z_0, s)$'s); therefore, the $K_{0,1}(z_0, s)$'s were modified at each value of z_0, independently of s. After the modifications we obtained better simulation results that fit the observed CVs very well (Figure 6). The CVs of some other $[XW_{12}O_{40}]^z$ (X = As, Ge, Co) were also fitted well (Table S2, Supporting Information). The $K_{0,1}(z_0, s)$ values finally used and the resulting protonation constants $K_{n,m}(z_0, s)$'s are given in Figure 7 and Table S3, Supporting Information, respectively. The values of $K_{0,1}(z_0, s)$ for $z_0 = -3$ and −5 coincide rather well with those predicted by eq 28′ using $K_{0,1}(-4, s)$ as a reference point, but the deviation from the value calculated becomes larger when $z_0 = -2$ or −6 (Figure 7). This deviation may be due to an unconsidered effect, such as a solvent leveling effect.[37] Diffusion constants of Keggin POMs and proton were also adjusted, but they affected not the shapes but the current intensities of the CVs.[38] The diffusion constants used are shown in Table 3.

The values become smaller as the ionic charge becomes negatively larger, being comparable to those reported previously.[14,15]

As for the mathematical expression of $\Delta G_p^{os}(H_m\langle n\rangle_s)$, we tested the following two formulas as well

$$\Delta G_p^{os}(H_m\langle n\rangle_s) = -C_p^s\cdot(m-1)\cdot s\cdot n \quad (26')$$

DOI: 10.1021/ic502970q
Inorg. Chem. 2015, 54, 2793−2801

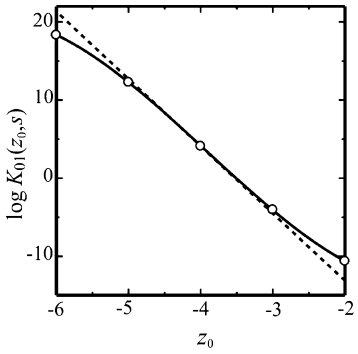

Figure 7. Plot of $K_{0,1}(z_0, s)$ used in the digital simulation (open circles). Dotted line shows $K_{0,1}(z_0, s)$ values systematically evaluated by eq 28′.

Table 3. Diffusion Constants Used in the Digital Simulation

X	z_0	D (without H^+)[a]	D (with H^+)[b]
S	−2	1.0×10^{-5}	1.1×10^{-5}
P	−3	9.0×10^{-6}	1.1×10^{-5}
Si	−4	7.0×10^{-6}	1.1×10^{-5}
B	−5	7.0×10^{-6}	8.0×10^{-6}
Al	−5	7.0×10^{-6}	8.0×10^{-6}
Ga	−5	7.0×10^{-6}	8.0×10^{-6}
Zn	−6	4.5×10^{-6}	7.5×10^{-6}

[a]The values in neutral acetonitrile. [b]The values in acidified acetonitrile. The unit is in $cm^2 \cdot s^{-1}$. The diffusion constant used for H^+ is 2.2×10^{-5} $cm^2 \cdot s^{-1}$.

and

$$\Delta G_p^{\circ s}(H_m\langle n\rangle_s) = -C_p^{s\prime} \cdot s \cdot n \qquad (26'')$$

39

The former formula reproduced the redox behaviors of the Keggin tungstate POMs roughly but was not suitable for systematic fitting for all Keggin POMs studied. The latter gave a rather good fitting but was inferior to eq 26 in describing the four-electron-like transfer of $[ZnW_{12}O_{40}]^{6-}$, as shown in Figure S2, Supporting Information. Nevertheless, the simulation based on the above three formulas (especially eq 26) described well the merging of two two-electron waves into a four-electron-like wave. Therefore, we suggest that the synergistic electron-withdrawing effect of the central μ_4-oxygens, pushed against the W atoms on the Keggin shell, and the protons, attached to the oxygens on the shell, should facilitate the electron transfer and leads to a redox-potential inversion (i.e., multielectron transfers).

4. CONCLUDING REMARKS

By discussion of the redox processes of various Keggin tungstate POMs on the basis of a electrothermodynamical model dealing with "simple" and "synergistic" electron-withdrawing effects (concerning s) of the μ_4-oxygens,[40] a perfect simulation of their CVs (i.e., simulation of the conversion from one-electron transfer to four-electron transfer via two-electron transfer) was achieved. The quite good reproduction achieved by the model proved the following: (1) s remains unchanged even when electrons are added to the Keggin POM; (2) consequently, in unacidified solvent, all potentials of the first to fourth redox waves are likewise shifted in the positive potential side, depending on s, and (3) in acidified solvent, the additional synergistic electron-withdrawing effect makes electron transfer easier and enables redox-potential inversions leading to multielectron transfer. These three findings are all related to the structural features of Keggin POMs, where an oxoanion (containing μ_4-oxygens) is cooped up in the rigid and stable POM shell having an inner space of a fixed volume. The multielectron transfer studied in the present work should be categorized into a proton-coupled electron transfer (PCET)[41−44] but is special in that the degree of potential inversion is accelerated depending on s. Thus, it is regarded as a new type of PCET that is derived from the structural features where highly electronegative species are cooped up in a "rigid and stable" closed shell. This finding will be a major clue in developing novel redox complexes (e.g., fullerene-based compounds) exhibiting multielectron transfers, which have similar structural features to the Keggin.

Furthermore, from the present study we obtained important findings about LUMOs of Keggin tungstate POMs. According to the findings, the first and second electrons occupy the orbitals lying at the same level, while the third and fourth electrons occupy the orbitals lying at a level higher by 0.2 eV than the levels of the first and second electrons. When additionally considering the known fact that the two-electron reduced Keggin POM exhibits diamagnetism, it is suggested that the doubly degenerate LUMO of Keggin POM having a point symmetry of T_d is split into two different energy levels separated by 0.20 eV and that the four added electrons occupy sequentially the two split energy levels from the bottom adopting a low-spin configuration. Furthermore, the on-site repulsion is suggested to be not large and regarded as equal to off-site repulsion. The close energy levels and the small on-site repulsion of LUMOs (or LUMO+1) for the Keggin POMs are important factors that enable four-electron transfer. More than four-electron transfer would be feasible if a complex possesses more than two LUMOs with close energy level and a small on-site repulsion.

■ ASSOCIATED CONTENT

Ⓢ Supporting Information

Protonation constants (calculated in the simulation), crystallographic data (used for calculating s values), redox potentials (observed and calculated), E_1 vs s plot and CVs (simulated by using eq 26″). This material is available free of charge via the Internet at http://pubs.acs.org.

■ AUTHOR INFORMATION

Corresponding Author

*E-mail: eda@kobe-u.ac.jp.

Notes

The authors declare no competing financial interest.

■ ACKNOWLEDGMENTS

The authors thank Prof. Emeritus Dr. Sadayuki Himeno and Ms. Kiyomi Nakajima for provision of CV data and their helpful discussion.

■ REFERENCES

(1) Zusman, L. D.; Beratan, D. N. *J. Chem. Phys.* **1996**, *105*, 165−176.
(2) Obare, S. O.; Ito, T.; Meyer, G. J. *J. Am. Chem. Soc.* **2006**, *128*, 712−713.
(3) Sumliner, J. M.; Lv, H.; Fielden, J.; Geletii, Y. V.; Hill, C. L. *Eur. J. Inorg. Chem.* **2014**, 635−644.
(4) Mizuno, N.; Misono, M. *Chem. Rev.* **1998**, *98*, 199−218.

DOI: 10.1021/ic502970q
Inorg. Chem. 2015, 54, 2793−2801

(5) Sadakane, M.; Steckhan, E. *Chem. Rev.* **1998**, *98*, 219−237.
(6) Rhule, J. T.; Hill, C. L.; Judd, D. A. *Chem. Rev.* **1998**, *98*, 327−357.
(7) Howells, A. R.; Sankarraj, A.; Shannon, C. *J. Am. Chem. Soc.* **2004**, *126*, 12258−12259.
(8) Pope, M. T.; Varga, G. M., Jr. *Inorg. Chem.* **1966**, *5*, 1249−1254.
(9) Pope, M. T. *Heteropoly and Isopoly Oxometalates*; Springer-Verlag: Berlin, 1983.
(10) Maeda, K.; Katano, H.; Osakai, T.; Himeno, S.; Saito, A. *J. Electroanal. Chem.* **1995**, *389*, 167−173.
(11) Zhang, J.; Bond, A. M.; Richardt, P. J. S.; Wedd, A. G. *Inorg. Chem.* **2004**, *43*, 8263−8271.
(12) Barrows, J. N.; Pope, M. T. *Adv. Chem. Ser.* **1990**, *226*, 403−417.
(13) Maeda, K.; Himeno, S.; Osakai, T.; Saito, A.; Hori, T. *J. Electroanal. Chem.* **1994**, *364*, 149−154.
(14) Prenzler, P. D.; Boskovic, C.; Bond, A. M.; Wedd, A. G. *Anal. Chem.* **1999**, *71*, 3650−3656.
(15) Himeno, S.; Takamoto, M.; Santo, R.; Ichimura, A. *Bull. Chem. Soc. Jpn.* **2005**, *78*, 95−100.
(16) Gao, G.-G.; Xu, L.; Wang, W.-J.; Qu, X.-S.; Liu, H.; Yang, Y.-Y. *Inorg. Chem.* **2008**, *47*, 2325−2333.
(17) Nakajima, K.; Eda, K.; Himeno, S. *Inorg. Chem.* **2010**, *49*, 5212−5215.
(18) Feldberg, S. W. In *Electroanalytical Chemistry*; Bard, A. J., Ed.; Marcel Dekker: New York, 1969; Vol. 3, pp 199−296.
(19) Bard, A. J.; Faulkner, L. R. *Electrochemistry Methods, Fundamentals and Applications*, 2nd ed.; Wiley: New York, 2001; pp 785−807.
(20) Brown, I. D.; Altermatt, D. *Acta Crystallogr.* **1985**, *B41*, 244−247.
(21) Mbomekallé, I.-M.; López, X.; Poblet, J. M.; Sécheresse, F.; Keita, B.; Nadjo, L. *Inorg. Chem.* **2010**, *49*, 7001−7006.
(22) In the quantum-mechanical study the influence of the heteroatom size on the redox potentials of Keggin anions was discussed as a function of the charge density on XO_4 fragments (or electrostatic potential produced by XO_4 fragments), which might correlate with *s* because of the constant sum of $X-\mu_4$-O and μ_4-O−W bond lengths in the anions, that is, shorter $X-\mu_4$-O bonds lead to longer μ_4-O−W bond distances. While a more negative potential produced by XO_4 and thus a negative shift in the redox potential of the Keggin anion were from the shorter μ_4-O−W bond in Mbomekallé's calculation, the same shift in the redox potential was from smaller *s* (i.e., the longer μ_4-O−W bond distance) in our model.
(23) The bond valence *s* of the bonds is defined as the number of bonding electrons per bond and is thus concerned with the depopulation on the W atom.
(24) Pauling, L. *The Nature of the Chemical Bond*, 3rd ed.; Cornell University Press: Ithaca, 1960.
(25) Cotton, F. A.; Wilkinson, G. *Advanced Inorganic Chemistry*, 5th ed.; A Wiley-Interscience Publication: New York, 1988.
(26) Huheey, J. E.; Keiter, E. A.; Keiter, R. L. *Inorganic Chemistry—principles of structure and reactivity*, 4th ed.; Harper Collins: New York, 1993.
(27) Osakai, T.; Maeda, K.; Ebina, K.; Hayamizu, H.; Hoshino, M.; Muto, K.; Himeno, S. *Bull. Chem. Soc. Jpn.* **1997**, *70*, 2473−2481.
(28) Murakami, W.; Eda, K.; Yamamoto, M.; Osakai, T. *Bull. Chem. Soc. Jpn.* **2014**, *87*, 403−411.
(29) Born, M. *Z. Phys.* **1920**, *1*, 45−48.
(30) Maestre, J. M.; Lopez, X.; Bo, C.; Poblet, J.-M.; Casañ-Pastor, N. *J. Am. Chem. Soc.* **2001**, *123*, 3749−3758.
(31) To be exact it should be mentioned that the on-site repulsion is larger than the off-site repulsion by 0.2 eV, because the contribution due to the off-site one is treated in ΔG_{eg}^{oz} and removed from ΔG_{eg}^{oorb}.
(32) Casañ-Pastor, N.; Baker, L. C. W. *J. Am. Chem. Soc.* **1992**, *114*, 10384−10394.
(33) This term is a function of the ionic charge that the Keggin anion has before the corresponding protonation.
(34) Actually the effect of the Coulomb interaction between the proton attached and the effective charge due to the electron depopulation is not large and may be ignored, because the proton is not directly attached to the W atom.
(35) Kozhevnikov, I. V.; Sinnema, A.; Jansen, R. J. J.; van Bekkum, H. *Catal. Lett.* **1994**, *27*, 187−197.
(36) Since the Keggin anions exhibit protonation at an ionic charge of −4, as mentioned above, the protonation constant $K_{0,1}(-4,s)$ was chosen as a fitting parameter (i.e., a reference point for systematic calculation of the other protonation constants used).
(37) Shriver, D. F.; Atkins, P. W. *Inorganic Chemistry*, 3rd ed.; Oxford University Press: Oxford, 1999.
(38) The peak current intensity of the CV was fitted by adjusting the diffusion constant of the Keggin POM anion.
(39) Since $\Delta G_p^{os}(H_m\langle n\rangle_s) = \Delta_f G^{os}(H_m\langle n\rangle_s) - \Delta_f G^{os}(H_{m-1}\langle n\rangle_s)$ (where $\Delta_f G^{os}()$ is a *s*-dependent part of the formation Gibbs energy of a species in parentheses), consequently $\Delta_f G^{os}(H_m\langle n\rangle)$ includes a term proportional to the product of $-m{\cdot}s{\cdot}n$, which is concerned with the synergistic effect.
(40) In the present work we found a significant correlation of the redox potential of the Keggin tungstate anion with the bond valence *s* of μ_4-O−W (specifically, larger *s* leads to a positive shift of the redox potential). When regarding the reduction as the electron gaining a W atom, such a positive shift is simply interpreted as an effect of the electron depopulation or of a less negative electric field (i.e., a less negative electrostatic potential produced by the XO_4 anionic entity) at the W atom. We tentatively proposed that the origin of the above correlation is an electron-withdrawing effect of μ_4-O based on the following reasons: (1) the bond valence *s* is a better controlling parameter of the redox potential than the electrostatic potential (see ref 21), (2) in a general concept of the bond valence for a W−O bond, electrons used for bonding the O and W atoms are regarded as to be drawn from the W atoms (i.e., *s* is related to withdrawing electrons from the W atom), and (3) the concept of electron withdrawing by the O atom seems suitable to build the synergistic effect that is mentioned and described with the product of $m{\cdot}s{\cdot}n$ in this paper. Because the electron depopulation at the W atom has not yet been confirmed, further discussing the origin of the correlation is necessary. There may be a sophisticated idea of the origin, alternative to electron withdrawing.
(41) Huynh, M. H. V.; Meyer, T. J. *Chem. Rev.* **2007**, *107*, 5004−5064.
(42) Evans, D. H. *Chem. Rev.* **2008**, *108*, 2113−2144.
(43) Schrauben, J. N.; Hayoun, R.; Valdez, C. N.; Braten, M.; Fridley, L.; Mayer, J. M. *Science* **2012**, *336*, 1298−1301.
(44) Kretchmer, J. S.; Muller, T. F., III *J. Chem. Phys.* **2013**, *138*, 134109.

DOI: 10.1021/ic502970q
Inorg. Chem. 2015, 54, 2793−2801